Dynamic behaviour of steel moment-resisting frames with a concrete slab on metal sheeting

Comportamento dinamico di telai in acciaio a nodi rigidi con soletta collaborante in calcestruzzo

This paper reports on a study on the dynamic behaviour of steel moment resisting frames with a concrete slab on metal sheeting. The experimental analysis, which is herein summarized, consists of two different series of tests: 1) component tests on beam-to-column joints under quasi-static cyclic reversal loading and 2) dynamic tests of complete full scale framed structures on the shaking table. Performance of joints and main parameters affecting their response are identified and discussed. Experimental results are also considered with reference to low-cycle fatigue behaviour and the associated fatigue resistance line are presented. Moreover, the performance of the joints in the frame under dynamic loading is analyzed and a simplified approach, which can be used for design purposes, is applied to monitor the damage accumulation process in steel framed structures under seismic action.

Questa nota propone uno studio sul comportamento dinamico di telai in acciaio con soletta in calcestruzzo gettata su lamiera grecata. L'analisi sperimentale, di seguito presentata in sintesi, ha previsto due differenti tipi di prove: prove sulla componente giunto trave-colonna in presenza di azioni cicliche alternate di tipo quasi statico e prove su tavola vibrante di sistemi intelaiati a grandezza reale. Il comportamento dei giunti ed i principali parametri che ne caratterizzano la risposta sono identificati e discussi.

I risultati sperimentali sono proposti con riferimento al fenomeno della fatica oligo-ciclica e vengono presentate le relative curve di resistenza a fatica. Viene inoltre analizzato il comportamento del giunto trave-colonna ed è proposto un approccio semplificato, utilizzabile a livello progettuale, per tenere in conto l' accumulo del danno in sistemi intelaiati in acciaio in presenza di azione sismica.

Prof. dr. ing. Carlo A. Castiglioni, prof. dr. ing. Claudio Bernuzzi
Structural Engineering Department, Politecnico di Milano, Milano, Italy
Prof. Panayotis Gr. Carydis
Laboratory for Earthquake Engineering, National Technical University of Athens, Greece

1. INTRODUCTION

Moment-resisting (MR) steel frames are usually designed in accordance with the capacity design philosophy, i.e., by assuming that the structural system has to provide sufficient strength, ductility and energy dissipation capabilities to resist severe earthquake, despite being severely damaged [1]. As pointed out in ref. [2], recent researches, which were carried out in the last decades on nodes of MR frames, permitted to develop a satisfactory knowledge on joint cyclic behaviour [3-5]. As a consequence, modern seismic provisions require that dissipation occurs at the beam ends and, eventually, at the base section of the columns. Nodal zones should hence embody sufficient strength and rotational stiffness so as to allow yielding as well as strain hardening in the dissipative zones, without any brittle fracture of structural components. During Northridge (1994) and Kobe (1995) earthquakes, a lot of MR frames suffered local damages in beam-to-column joints [6–8]. Unprecedented combined phenomena (i.e., notch effect due to backing bars, lack of preheating for thick flange plates and inadequate workmanship and inspection) appeared as key factors responsible for the severe failure modes of joints. Moreover, high strain rate effects, associated with ground motion, generated material overstrength and, as a consequence, joint ductility resulted remarkably reduced. Several studies [2] were hence carried out to explain both fracture locations and failure modes, which were observed during the aforementioned earthquakes. It has been hence underlined the importance and the need of efficient design approaches, based on the possibility of predicting accurately the response of beam-to-column joints in terms of hysteretic behaviour as well as of cumulated damage and failure. As a consequence of these unexpected failures, a great number of research programs were undertaken, all over the world, in order to:

- investigate the behaviour of typical connections used in MR frames under seismic loading;
- identify new connection typologies, developing a ductile behaviour under an earthquake;
- set up safe design rules for new structures in seismic areas;
- propose suitable damage assessment methods and repair procedures to be adopted in engineering practice.

This paper deals with a part of the research, which is currently in progress at the Politecnico of Milano in co-operation with the University of Athens (GR), aimed to assess the validity of the linear approach for seismic design[20, 23, 24] based on the "component behavior" [9,10], which has been up-to-now presented in the literature with reference to isolated structural components (beams, columns, joints). Owing to the influence of joints in MR steel frames, the first part of the experimental analysis comprised joint tests. Key

aspects of the behavior of this component are in the following presented and discussed, by considering also the influence on the joint performance due to the presence of a concrete slab on metal sheeting. Furthermore, the results associated with the second experimental phase of the study, i.e., shaking table tests of complete framed systems are proposed and joint action in the overall frame is analyzed. Finally a simplified approach is shortly presented and applied, which has been developed for the study of the damage accumulation process and can be used for practical design purposes in the field of steel as well as steel-concrete composite frames.

2. THE RESEARCH PROGRAMME

Design analysis of frames in seismic zones, is usually carried out by means of two alternative method: a) non linear dynamic analysis under real or synthetic accelerograms or b) linear dynamic analysis to verify the safety of the structure based on its response to a design spectrum. For its simplicity, the second method is the most frequently used for building design. It implies the definition of the design response spectrum by means of the use of behaviour factor (q-factor), which embodies the non-linear dissipative characteristics of the actual structure. Following this approach, the horizontal design forces simulating earthquake actions are obtained by means of suitable response spectra, which give the design acceleration as a function of the damping factor (ξ) and the natural period (T). In recent seismic Codes [11-13], the generic design response spectrum $S_a(T,\xi)$ is expressed as:

$$S_a(T,\xi) = a_0 [R(T,\xi)/q] \quad (1)$$

where $R(T,\xi)$ is the response spectrum normalised to a peak ground acceleration of 1.0g, (obtained by modelling the structure as a linear elastic dynamic system) and a_0 represents the maximum peak ground acceleration expected in the site in exam.

Modern seismic provisions, propose q-factor values, usually aimed at the definition of the maximum ductility, depending only on frame typology, geometrical regularity, ductility of member as well as of joints [1]. These q values, which are generally based on monotonic analyses, allow the adoption of simplified linear elastic design methods, but they appear in many cases unable to represent the actual frame performance in terms of the energy dissipation capacity, which depends strictly on several others factors (such as, material properties, geometry of frame components, degree of redundancy, buckling effects and deterioration of the mechanical properties of frame components/details). As showed by some recent studies [14,15], a more refined assessment of q-factor could not disregard the different limit states which the structures can achieve and, as a consequence, low-cycle fatigue limit state has to be considered, too. Cyclic performance as well as fatigue endurance life of frame dissipative components should consequently be determined by means of suitable experimental activities. The subsequent analysis of test results has to be hence finalized to identify the parameters to be used in the seismic design of the whole framed structure.

The present research is aimed at the study of the behaviour of MR frames with a concrete slab on metal sheeting. Owing to the influence of the behaviour of beam-to-column joints on the overall frame behaviour, the experimental analysis has been sub-divided in two series of tests:

- component tests on beam-to-column joints under quasi-static cyclic reversal loading. These tests have been executed at the Politecnico of Milan (I);
- full scale tests of complete frame structures on a shaking table, which have been carried out at the Laboratory of the National University of Athens (GR).

These two test series were executed in different steps. Initially, attention has been focused on beam-to-column joints. A multispecimen testing program on rigid joints has been carried out, on two different type of joints: 1) steel joints and 2) steel joints with a concrete slab on metal sheeting. Moreover, it should be noted that tests on full scale three-dimensional framed structures are aimed both to investigate the behaviour of the whole structural system as well as to analyze the damage accumulation process in the weaker components of the frame [16].

3 JOINT TEST RESULTS

The specimens considered for the joint experimental analysis consist of an IPE 160 beam attached to a HEB180 column by a welded connection. Two types of welds were considered: specimens type C1 are representative of a typical site welding, with single bevel V groove welds and a backing bar; specimens type C4 are representative of a typical shop welding, with double bevel K groove welds (Fig. 1). Two series of 6 specimens each were fabricated, representative of an external beam-to-column connection in a MR frame; hence the specimens were of the $\perp$ type.

The first set of specimens (named as "ns") consists of the sole steel beam-to-column connection; the second one, (identified as "s") encompassing the presence of a 100 mm r.c. slab, cast in a corrugated steel sheeting 55 mm deep (Fig. 2). The slab was connected to the steel beam only by means of three studs positioned near the free end of the beam, used only to prevent separation and detachment of the concrete slab from the beam end at the load application zone. Hence, the specimens cannot be considered as acting as

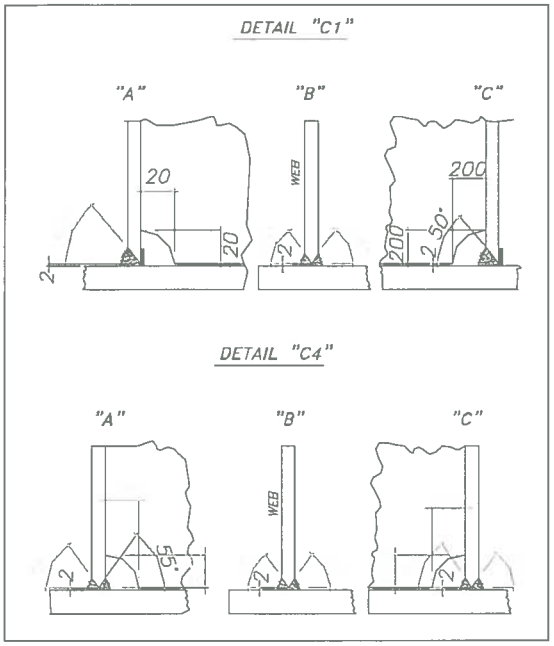

Fig. 1
Welding details of the steel beam-to-column joints.

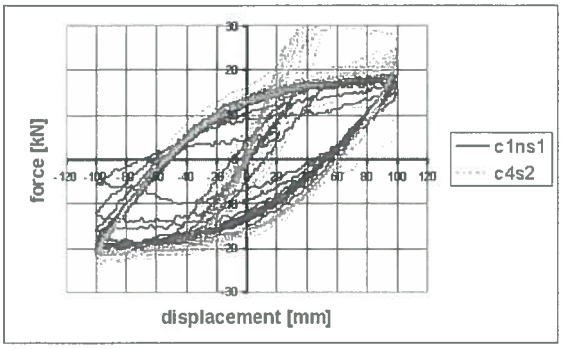

Fig. 4
Comparison of hysteresis loops for specimens with and without concrete slab.

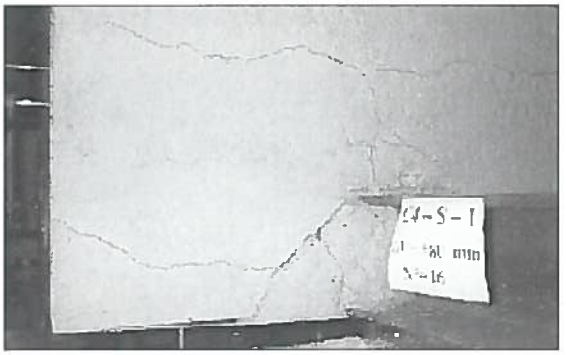

Fig. 5
Damage in the concrete slab.

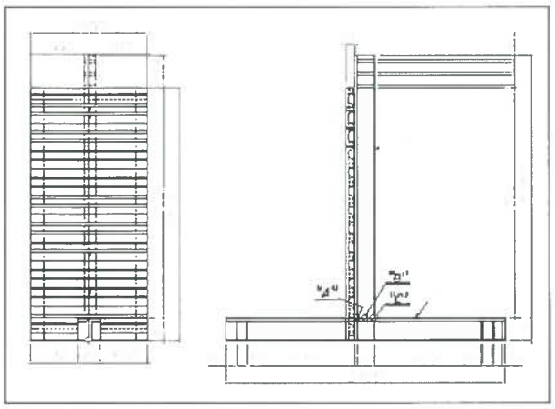

Fig. 2
Specimen of steel beam-to-column joint with the concrete slab on metal sheeting.

Specimen	Δv [mm]	v_y^s [mm]	F_y^s [kN]	v_y^c [mm]	F_y^c [kN]	Ntot.
C4-s-3	350	38.8	19.1	35.6	34.1	4
C4-s-2	200	36.2	22.9	30.0	29.1	17
C1-s-1	160	37.6	22.2	31.3	29.9	37
C1-s-2	140	35.8	22.9	30.6	29.2	56
C1-s-3	120	39.1	20.7	32.4	33.9	57

Table 1 - Test results for specimens with the concrete slab on metal sheeting.

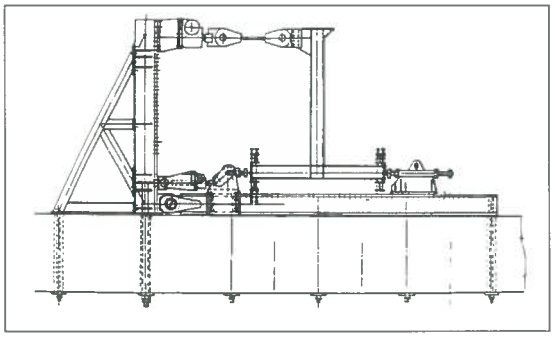

Fig. 3
Testing set-up designed by Ballio and Zandonini [17].

Specimen	Δv [mm]	v_y^s [mm]	F_y^s [kN]	Ntot.
C1-ns-2	300	41.4	18.6	5
C1-ns-3	240	43.3	18.8	22
C1-ns-1	200	43.0	19.1	25
C4-ns-1	160	39.9	18.4	51
C4-ns-2	120	41.6	18.8	73

Table 2: Test results for specimens without the slab.

composite, but the presence of the slab is considered only in order to simulate real structural conditions and to prevent local buckling of the upper flange of the beam. Of the 6 specimens of each series, three were welded according to the C1 detail, the other three according to the C4 detail. Only 5 specimens of each series have been tested at present; the sixth one with a C4 type connection was left intact, for eventual future experimental verifications.

Specimens of beam-to-column connection were tested by means of the equipment (Fig. 3) designed by Ballio and Zandonini [17]. During the test, the column is laying horizontally while the beam is standing in the vertical position, and subjected to an horizontal displacement imposed at the beam end by a jack governed by an electric engine.

In tables 1 and 2 key features of the joint tests are summarized, for specimens with and without concrete slab, respectively. Term Δv represents the displacement range imposed at the beam end, i.e. the assumed control test parameter, v_y^s and F_y^s are respectively the yield displacement and the yield strength in the case of hogging moment (concrete in tension), while v_y^c and F_y^c are respectively the yield displacement and the yield strength in the case of sagging moment (concrete in compression). These terms have been evaluated in accordance with the procedure proposed in the ECCS recommendations [18].

As a general remark, it can be said that specimens with the concrete slab, in the first cycles, when the con-

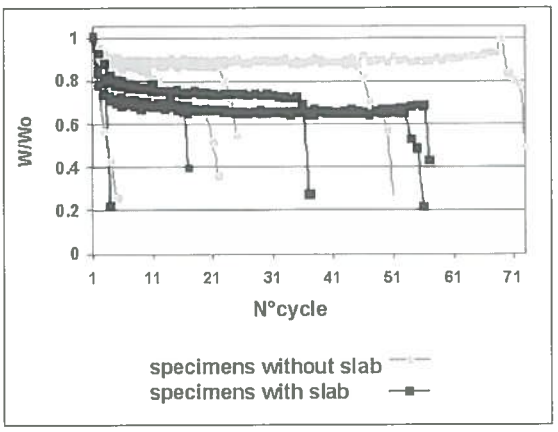

Fig. 6 Comparison of energy dissipation capacity for specimens with and without concrete slab.

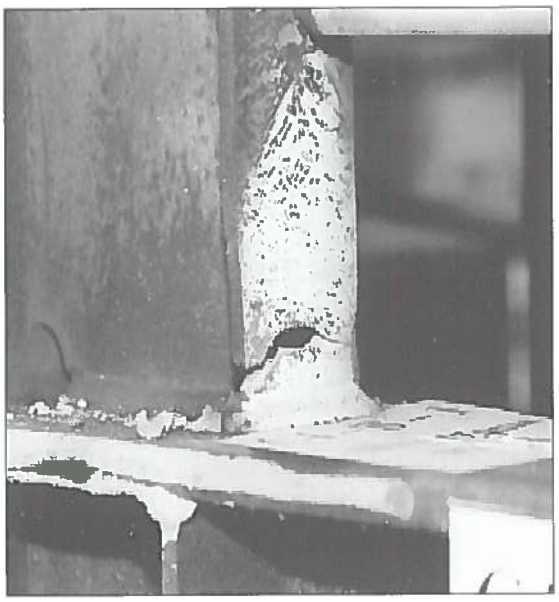

Fig. 7 Typical failure mode, with weld cracking.

crete in compression is undamaged, show a larger strength and stiffness than the corresponding ones made of steel only, owing to the influence both of adhesion and chemical bond and of the interface friction. As an example, figure 4 can be considered, where the comparison between the hysteresis loops for the two specimens C4-S-2 and C1-ns-1, that were tested under cycles of the same amplitude (200 mm) is presented. Furthermore, in case of joints with slab there is also an evident difference in stiffness between the case of sagging and hogging bending moment, due to action of concrete in compression. Immediately after the first large cycle beyond the elastic limit, the concrete slab cracked in compression. This fact was noticed also in specimens tested under smaller cycle amplitudes, as shown in figure 5, in the case of specimen C4-s-1. After cracking of the concrete, an evident reduction is observed in the specimen strength, which becomes comparable with that of corresponding specimen without slab.

Furthermore, energy absorption capabilities have been considered and figure 6 shows a comparison among the various specimens tested, in terms of dissipated energy per cycle (W) normalized over the value of the energy dissipated in the first stable cycle in the plastic range (W_0). It can be noticed that, in non dimensional terms, the specimens with the concrete slab show a clear deterioration in the first three to five cycles, followed by a stabilization and a rapid final stage of deterioration, leading to collapse. On the contrary, the specimens without the concrete slab do not evidence the initial deterioration stage, but show a rather stable behaviour, until a final stage is reached when rapid deterioration takes place, leading to collapse. These considerations can be applied to all the specimens, except for C4-s-3 and C1-ns-2, specimens, which were tested under very large amplitudes, that do not present any stabilization stage, but collapse in a few cycles (respectively, 4 and 5 cycles).

It is also evident (figure 6) that practically all the specimens tested collapsed in a "brittle" failure mode, that is without showing any steady deterioration but evidencing an abrupt deterioration only one or two cycles before complete failure, after a relatively long period in which the capacity of the specimen to dissipate energy remained nearly constant. As an example, figure 7 shows a failure mode that can be considered typical for all the specimens tested. Independently on the presence or absence of the concrete slab, failure was always attained by cracking at the welded joint, with limited buckling evidence in the beam flange. This confirms the already mentioned "brittleness" of the failure mode. In fact, the rather limited slenderness ratios of the web and flanges of the IPE 160 beam are such that the cycle amplitudes imposed to the specimens does not result in local buckling of the beam flanges and in the formation of a plastic hinge. This fact causes overloading of the welded joint and leads to its ("brittle") failure after a few cycles, as previously observed for steel joints by Castiglioni et al. [19, 24].

4. ANALYSIS OF JOINT TEST DATA

As proposed by Ballio and Castiglioni [20], fatigue endurance of steel components can be analysed via the S-N line approach, detail by means of the well-known relationship:

$$NS^m = K \qquad (2)$$

where S is a parameter selected to measure the level of damage or to assess failure (representative of the global effect of the imposed cyclic actions), N represents the number of cycles at collapse and terms m and K are constant parameters.

In the Log-Log domain, eq. 2) represents a straight line (fig. 8) defined as:

$$Log(N) = Log(K) - mLog(S) \qquad (3)$$

As to the choice of parameter S, reference should be conveniently made to global displacement parameters

(rotation, interstorey drift, displacement) instead of local deformation parameters as in case of high-cycle fatigue.
Some proposals for the definition of the parameter S and the associated value of exponent m, have been recently proposed [19], which are based on eq. 2). In the following as parameter S, the cycle amplitude both in terms of imposed displacement Δv at the beam end and nodal rotation $\Delta\Phi$ on the joint are considered, while m=3 was always assumed.
As to the definition of the Fatigue Endurance (N), in the following reference is also made to the "Relative Energy Drop Criterion" [21]. According to this criterion, failure occurs either when the relative energy drop, defined as:

$$\Delta W_r^i = (W_0 - W_i) / W_0 \qquad (4)$$

where W_i is the absorbed energy at i-th cycle, and W_0 is the energy absorbed in the first stable cycle in the plastic range.
Failure is conventionally identified by the last cycle beyond which there is an evident increment relatively to ΔW_r^{i-1} or by the last cycle of the loading history, if the energy drop is not remarkably evident).
Tables 3 and 4 summarise the tests results in terms of values for N_{tot}, the total number of cycles experimentally imposed to the specimen, and N_f is the number of cycles to failure according to the

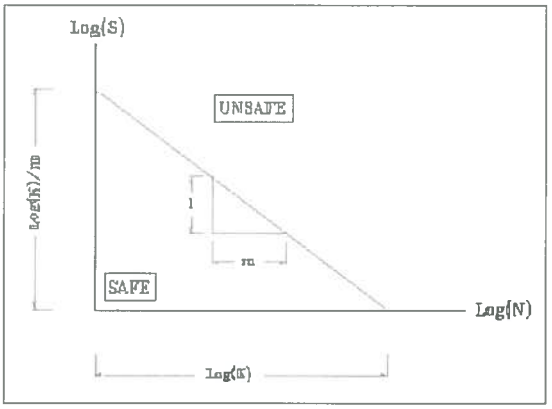

Fig. 8
Fatigue resistance line in Log(S)-Log(N) domain.

Specimen	Δv[mm]	$N_{tot.}$	N_f
C1-ns-2	300	5	5
C1-ns-3	240	22	20
C1-ns-1	200	25	22
C4-ns-1	160	51	45
C4-ns-2	120	73	69

Table 3
Layout of tests on specimens without slab.

Specimen	Δv[mm]	$N_{tot.}$	N_f
C4-s-3	350	4	3
C4-s-2	200	17	15
C1-s-1	160	37	35
C1-s-2	140	56	53
C1-s-3	120	57	56

Table 4
Layout of tests on specimens with slab.

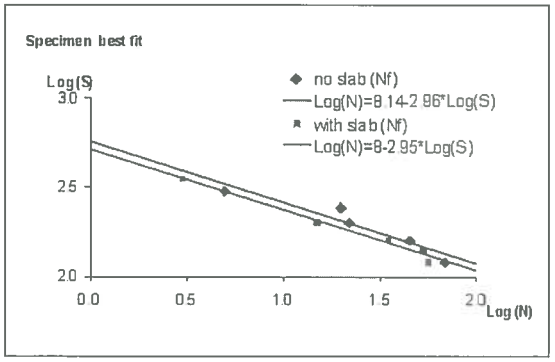

Fig. 9
Best fit S-N lines assuming S=Δv.

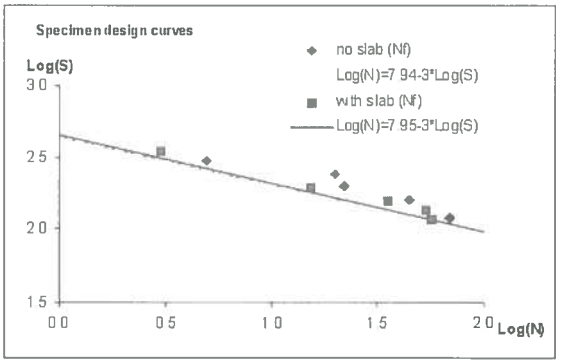

Fig. 10
Design S-N lines assuming S=Δv.

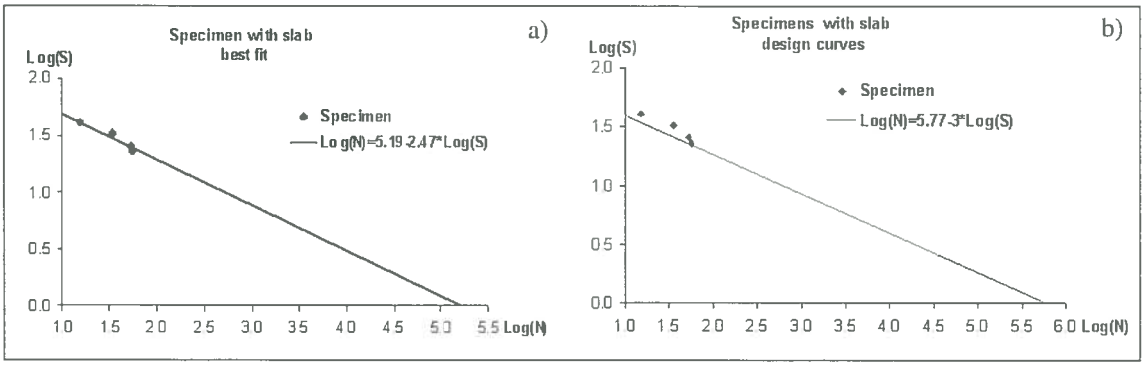

Fig. 11
S-N lines assuming S=ΔΦ for the cases of: a) experimental results and b) design curves.

"Relative Energy Drop". The S-N lines for the specimens were obtained assuming as parameter S the displacement range Δv and are presented in Figures 9 and 10, which report the best fit S-N line and the design S-N curve, respectively.
It can be noticed that the low-cycle fatigue strength of the specimens with the reinforced concrete slab is lower than the one of the specimens made of the steel profiles only. Figure 11 presents, for the specimens with slab, the S-N lines obtained by assuming as S the joint rotation $\Delta\Phi$ instead of the displacement range Δv. It must be noticed that changing the parameter to be assumed as S in eq. 2) a new definition of the constant K that appears in the S-N line equation is required.

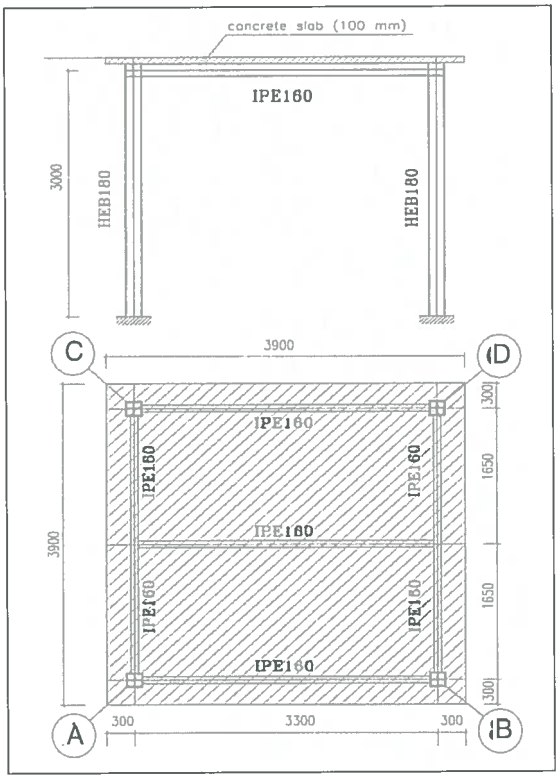

Fig. 12 The frame specimen for shanking table tests.

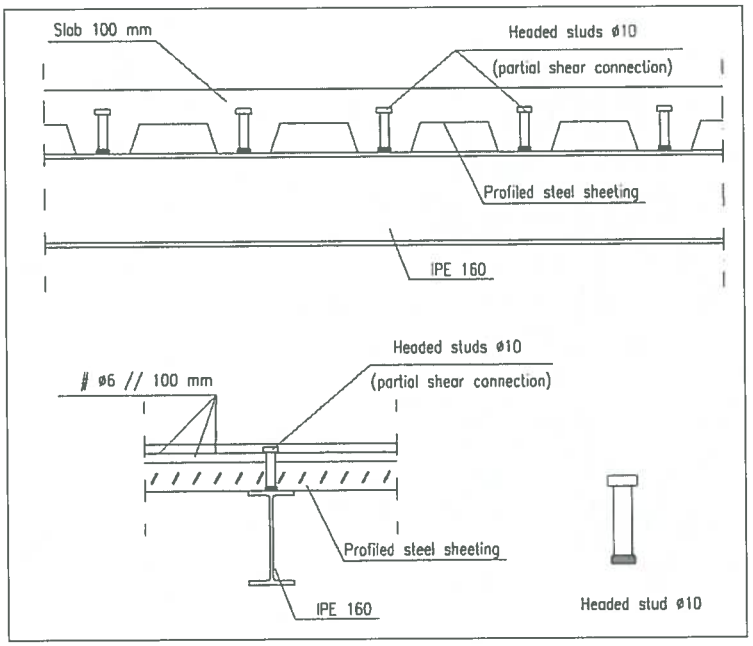

Fig. 13 Details of the composite steel beam and r.c. slab.

Table 5 Period and damping ratio of the tested frames.

SPECIMEN	Period (sec)	Frequency (Hz)	Damping (%)
STF3 1stud/1 rib	0.144	6.93	2.10
STF4 1stud/2 ribs	0.147	6.80	2.50

5. SHAKING TABLE TESTS OF COMPOSITE STEEL FRAMES

In order to verify the validity of the proposed approach for low-cycle fatigue damage assessment, dynamic tests were performed on two steel frames with a reinforced concrete (r.c.) slab, adopting for the beam-to-column connections and for the r.c. slab the same structural details and profiles of the joint specimens tested under cyclic quasi-static conditions. This allowed an analysis of the dynamic test data and evaluation of the damage index based on the same S-N lines previously obtained for the beam-to-column connections.

The dynamic tests were carried out at the shaking table facility of the Laboratory for Earthquake Engineering of the National Technical University of Athens. Although hereafter only the results of two dynamic tests on frames with welded beam-to-column connections are presented in order to allow the comparisons with the cyclic tests performed in Milano, the research carried out in Athens is much wider in scope, encompassing tests on two sets of 5 frames each, characterised by different structural details for the beam-to-column connections and the r.c. slab connection to the steel beam.

Figures 12 and 13 show the overall view of the tested frame specimen as well as the details of the connection of the r.c. slab to the beam, respectively. Tests were carried out on two similar frames, with HE180B columns in Fe 510 Steel and IPE 160 beams in Fe 360; the two frames, named STF3 and STF4 respectively were characterised by different connection details of the r.c. slab to the IPE160 beam: specimen STF3 was constructed with 1 stud ϕ10mm per rib of the steel sheeting, while in specimen STF4, 1 stud ϕ10mm every two ribs was adopted.

Table 5 summarises periods and damping factors computed by re-analysis of dynamic test results for the two specimens. The identification of these dynamic characteristics was performed by means of a sine logarithmic sweep base excitation, in a frequency range of 1-6 Hz, at the rate of one octave per minute. The damping factor was computed by using the half power bandwidth method.

Earthquake simulation tests were performed using a ramped sinusoidal excitations, with a frequency of 5 Hz, which is approximately equal to 80% of the own frequency of the specimens.

Each specimen was monitored by means of 7 accelerometers to record the acceleration in various points of the slab and of the steel frame, 4 displacement transducers for recording the absolute displacements of the frame, and 6 displacement transducers to record the relative displacements of the slab with respect to the steel beam (3 LVDTs on each beam) and 4 displacement transducers to record the relative rotations of the beams with respect to the columns (1 LVDT in each node).

Furthermore in two cross sections of one of the beams, 5 electrical strain gages were positioned in a line, in order to obtain, in each cross section, strains in the top and bottom flange, in two locations along the web and in the concrete slab; in addition, in two cross section along the height of the columns, half-bridged strain gages were placed on the column flanges in order to obtain bending moments.

These instrumented sections to be on the beams and the columns were chosen in positions where the behaviour could be predicted to remain linear elastic within the whole test duration.

The following figures 14-18 and 19-23 show, respectively for specimens STF3 and STF4, the acceleration

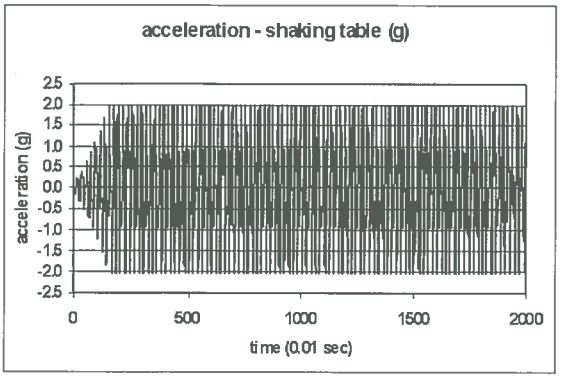

Fig.14a Acceleration of the shaking table vs. time for specimen STF3.

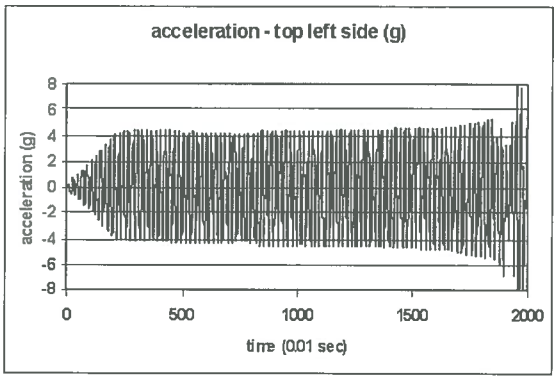

Fig. 14b Acceleration on top of the r.c. slab vs. time for specimen STF3.

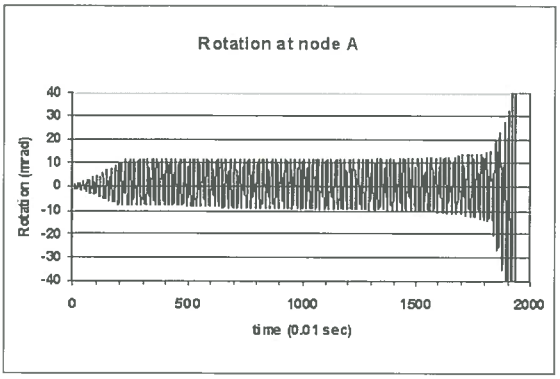

Fig. 15a Rotation vs. time at node A of specimen STF3.

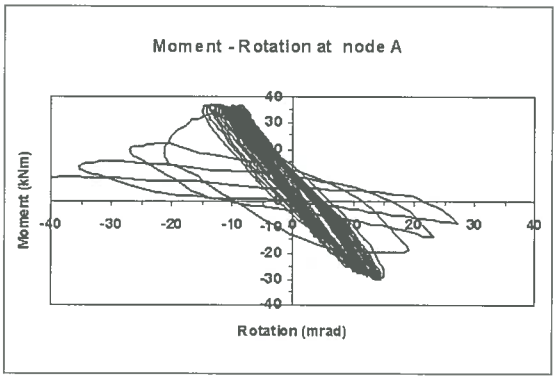

Fig. 15b Moment vs. rotation at node A of specimen STF3.

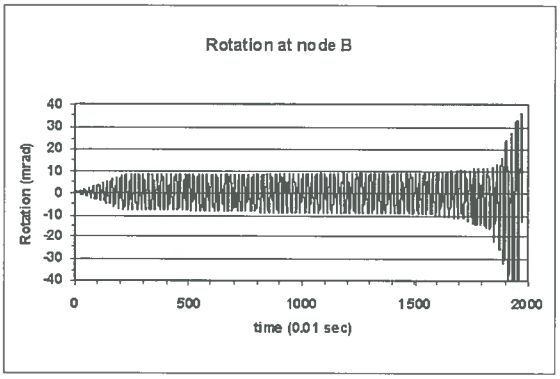

Fig. 16a Rotation vs. time at node B of specimen STF3.

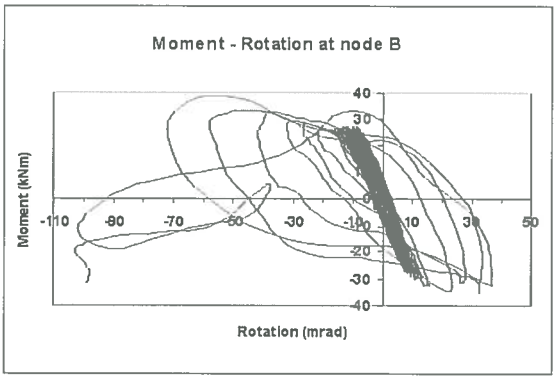

Fig. 16b Moment vs. rotation at node B of specimen STF3.

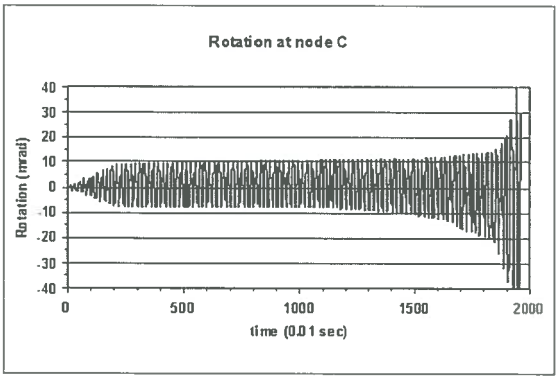

Fig. 17a Rotation vs. time at node C of specimen STF3.

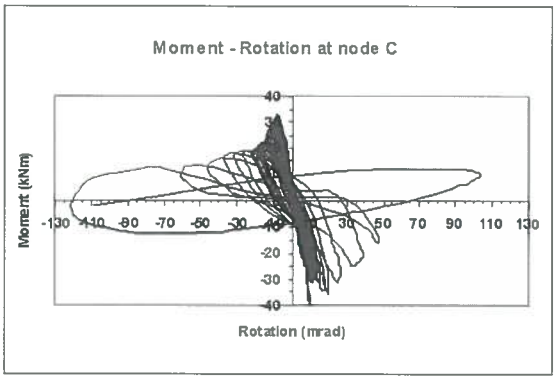

Fig. 17b Moment vs. rotation at node C of specimen STF3.

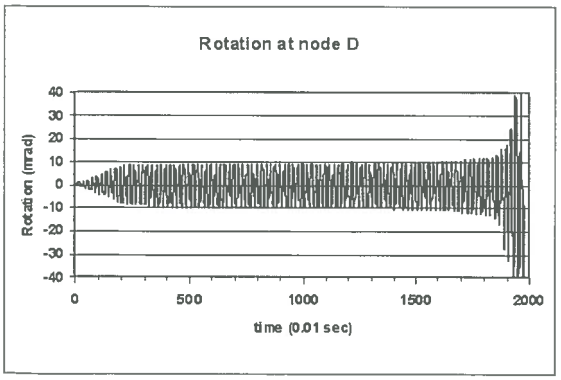

Fig. 18a Rotation vs. time at node D of specimen STF3.

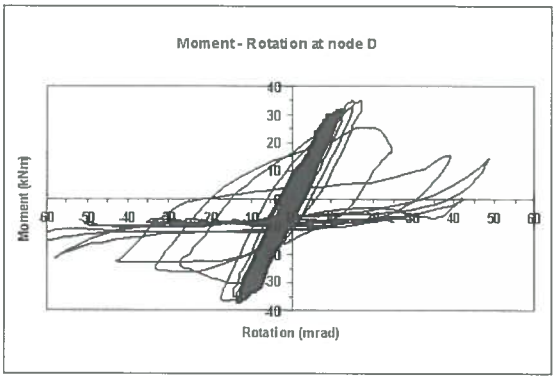

Fig. 18b Moment vs. rotation at node D of specimen STF3.

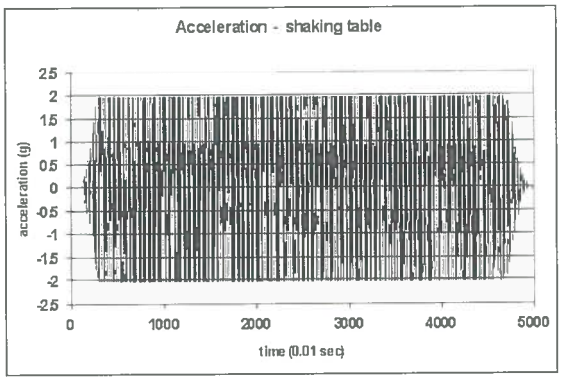

Fig.19a Acceleration of the shaking table vs. time for specimen STF4.

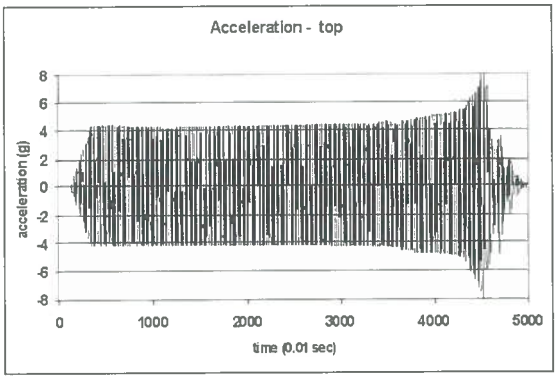

Fig. 19b Acceleration on top of the r.c. slab vs. time for specimen STF4.

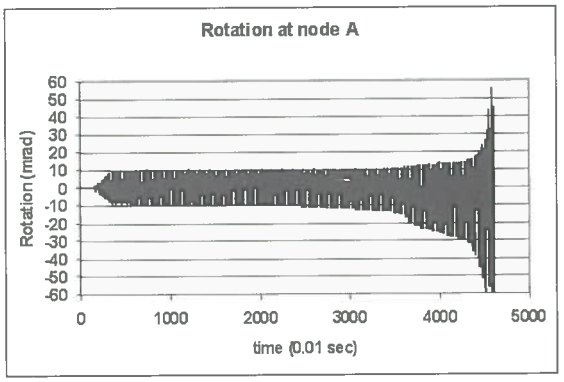

Fig. 20a Rotation vs. time at node A of specimen STF4.

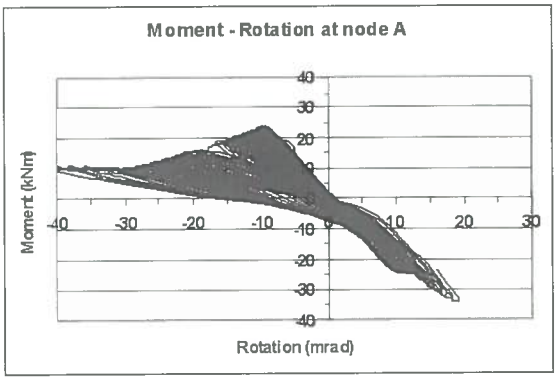

Fig. 20b Moment vs. rotation at node A of specimen STF4.

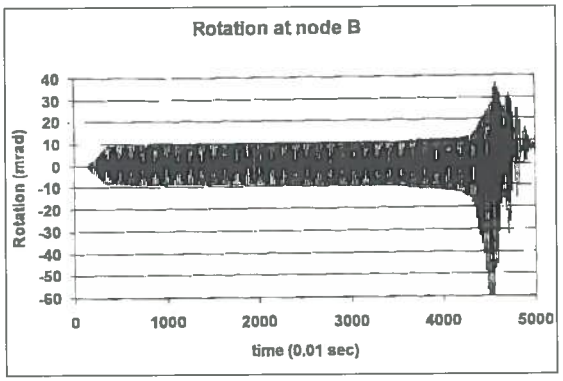

Fig. 21a Rotation vs. time at node B of specimen STF4.

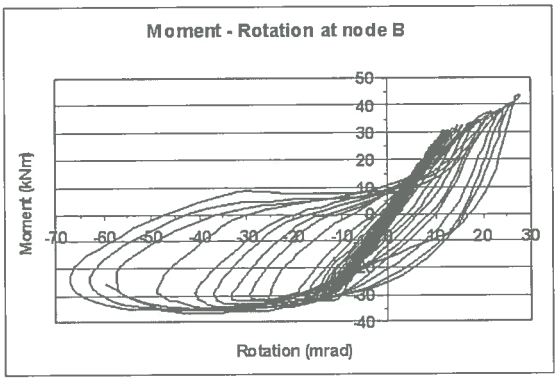

Fig. 21b Moment vs. rotation at node B of specimen STF4.

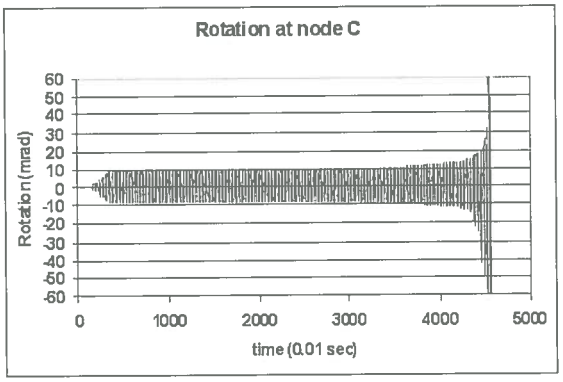

Fig. 22a Rotation vs. time at node C of specimen STF4.

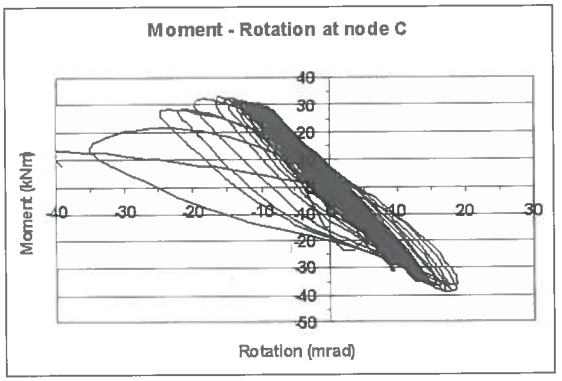

Fig. 22b Moment vs. rotation at node C of specimen STF4.

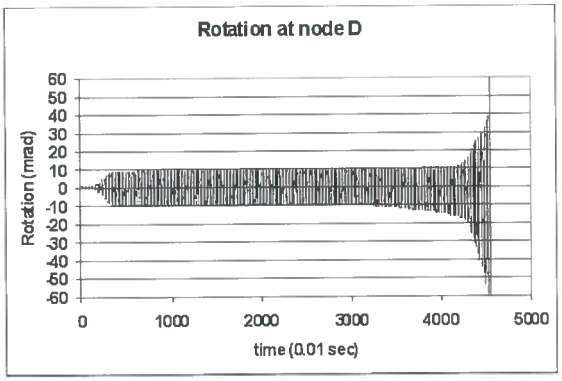

Fig. 23a Rotation vs. time at node D of specimen STF4.

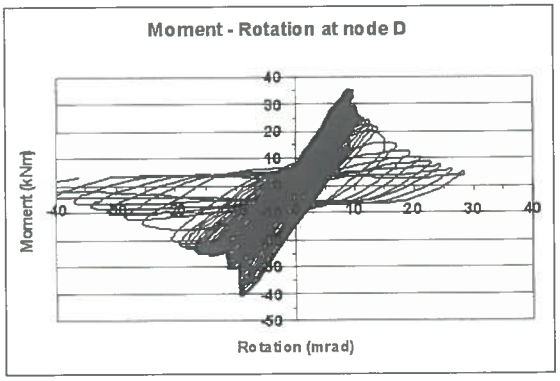

Fig. 23b Moment vs. rotation at node D of specimen STF4.

of the shaking table compared to that recorded on the top of the r.c. slab of the specimen (fig. 14 and 19), the relative rotations recorded between the beams and the columns at the four beam-to-column connections of the specimens and the moment-rotations diagrams for the same nodes (fig. 15-18 and 20-23). The bending moments plotted in these figures are to be considered as effective elastic bending moments and were obtained as a linear extrapolation of the values obtained by strain gauge recording in the instrumented cross sections of the beams and the columns.
It can be noticed that after nearly 18 seconds for specimen STF3 (fig. 14) and nearly 35 seconds for specimens STF4 (fig. 19), the acceleration recorded at the top of the r.c. slab begins to increase, while the input motion (i.e. the acceleration of the shaking table) remains constant. This fact indicates that some damage occurred in the structure. This is confirmed by examining the following figs. 15-18 and 20-23; these show that, corresponding to the noticed increase of the acceleration of the r.c. slab, also an increment in the relative rotation between the beams and the columns of the specimens occurs.
The hysteresis loops plotted in the same figures confirm that, after a phase during which the beam-to-column joints of the specimens exhibit practically a linear elastic behaviour, deterioration of both stiffness and load carrying capacity occurs, leading to complete failure of the connection.
For both specimens collapse occurred due to failure of all the four welded beam-to-column connections. Cracks always started at the lower flange of the beam and propagated upward, in some cases completely severing the beam web from the column flange. Such type of failures are similar to those reported in many MR steel frames in California during the Northridge earthquake, despite the size of the members that in this case are very small, due to the need of keeping the size of the model to an acceptable dimension for the shaking table facility.

6. LOW-CYCLE FATIGUE DAMAGE ASSESSMENT FOR DYNAMIC TEST SPECIMENS

Low cycle fatigue damage assessment was performed for the various beam-to-column connections of both specimens STF3 and STF4, based on Miner's rule [22] and the S-N lines previously obtained for the joints tested in Milano, under cyclic quasi-static conditions.
The moment-rotation time history for each node was re-analysed by means of the Rainflow cycle counting method in order to obtain the histogram (fig. 24) giving for each cycle amplitude the number of occurrences in the joint time-history.
Then the damage index was computed according to Miner's rule, making reference to the S-N lines derived in terms of rotations, i.e. assuming as parameter S the relative rotation of the beam to the column (fig. 11b).

Fig. 24
Cycle amplitudes at the joints of frame STF3.

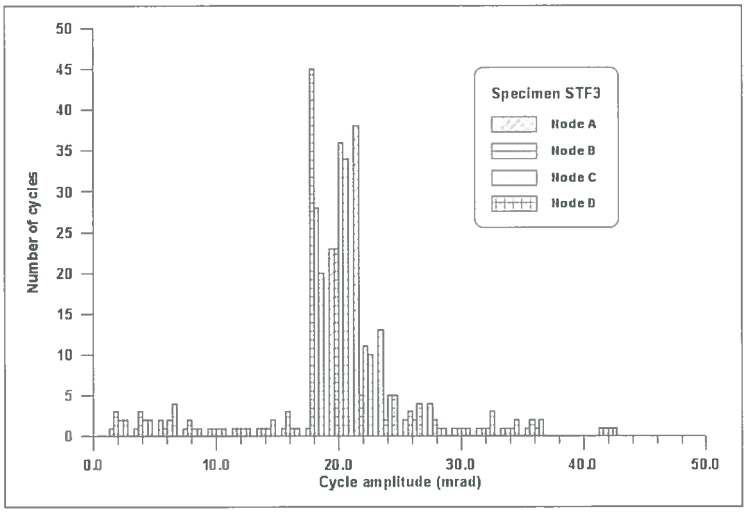

The following figs. 25 and 26 show, respectively for specimens STF3 and STF4 how the damage cumulates in the various nodes of each specimen.
Of course, due to the Rainflow cycle counting procedure, it is not possible to compare the damage accumulation with the real time, because Rainflow reorders the actual cycle sequence, and produces a sequence of cycles ordered for increasing cycle amplitude, independently of the real time-history (fig. 24).

Fig. 25a and fig. 26a show, respectively for specimens STF3 and STF4, how the damage index increases with the number of cycles imposed to the specimen, while figs. 25b and 26b propose the dependence of the cumulative damage index on the cycle amplitude: in fact, it is evident that cycles amplitudes smaller than 15 mrad practically leave the joints undamaged. For both specimens, it can be noticed that collapse is caused by those cycles with amplitudes ranging from 15 to 22 mrad, i.e. by those cycles having amplitudes nearly 3 to 4 times the yield rotation. It fact, it is corresponding to cycles having this amplitude that the cumulative damage index attains a value of unity.

From examining the same figures as well as the previous fig. 24, it is evident that most of the cycles

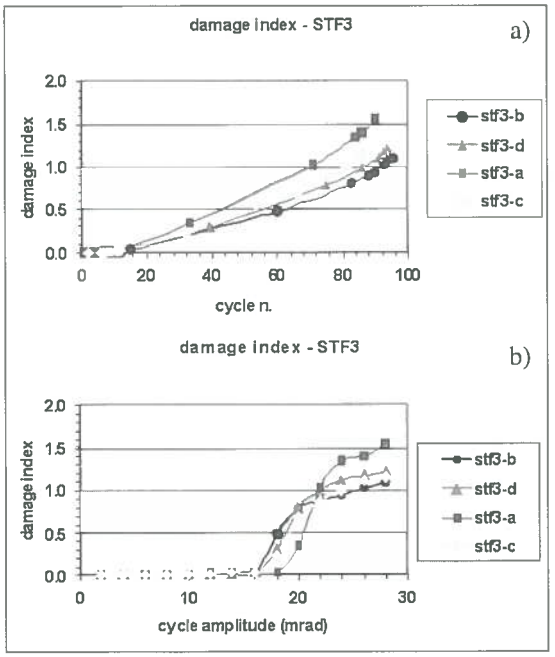

Fig. 25
Damage accumulation process for frame STF3:
a) damage index versus the number of executed cycles and
b) damage index versus the cycle amplitude.

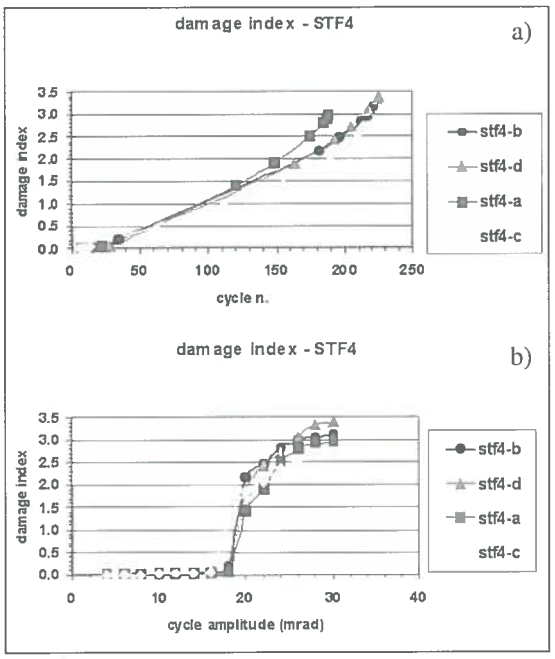

Fig. 26
Damage accumulation process for frame STF4:
a) damage index versus the number of executed cycles and
b) damage index versus the cycle amplitude.

imposed to the specimen had a rotation amplitude around 20 mrad, and that larger amplitude cycles occurred only after collapse of the joint. This confirms that the cause of the values of the damage index larger than 1.0, that can be noticed in fig. 25 and 26, is the fact that although the test was stopped at failure of the first joint, a few cycles of oscillation of the structure occurred, inducing in the already damaged nodes very large relative beam-to-column rotations.
Examining these figures, however, it can be concluded that the proposed damage assessment procedure allows a correct interpretation of the physical reality, in fact the results obtained for both specimens in terms of damage index are absolutely compatible with a definition of failure of the connection in good agreement with the experimental evidence.

7. CONCLUSIONS

An experimental study was carried out on MR steel frames, which comprised both component and full scale tests. As to the beam-to-column joint tests, some specimens consisted only of the steel profiles, others had also a r.c. slab. The specimens were subjected to cyclic quasi-static constant amplitude displacement histories. Failure was always attained in a brittle mode, by fracture of the welds between the beam and the column flange. In the presence of the slab, failure was always attained at the lower flange. Test data were re-analyzed in order to assess the low-cycle fatigue strength of these structural details, according to a proposal by Ballio and Castiglioni [20], and adopting the failure criteria presented in this paper. It is shown that the failure criterion proposed by Castiglioni [16,23] as well as the proposal by Castiglioni et al [24] give conservative results, that can lead to close estimates (a-priori) of the actual failure conditions, both in terms of number of cycles to failure and of energy dissipation capacity of the specimen. Test results evidenced that the presence of the concrete slab reduces the low-cycle fatigue strength of the specimens. This fact is probably due to the increment of strains in the lower flange caused by the shift upward of the neutral axis in the presence of the concrete slab.
Results of dynamic tests on full scale frame specimens are in good agreement with those of cyclic quasi-static tests on joints. In particular, they confirmed the validity of a seismic damage assessment procedure based on S-N lines (expressed in terms of global displacement components) and of a linear damage accumulation model (e.g Miner's Rule).
Despite the size of the specimens, that had to be kept limited due to the shaking table capacity, the experimental results showed failure modes for the beam-to-column joints similar to those reported after Northridge and Kobe earthquakes, in structures with large size members and joints.

ACKNOWLEDGEMENT

Authors wishes to acknowledge the financial support to this research by the Italian Ministry of University and Research (MURST), Cofinanziamento 1997 e 1999, by the Italian Consiglio Nazionale delle Ricerche (CNR) and of EU (within the TMR Access to Large Scale Testing Facility program). The skilfulness of dr. Ing. H. Mouzakis and of the whole technical group at LEE-NTUA, is deeply acknowledged.

REFERENCES

[1] Mazzolani F.M., Piluso V., 1996, Theory and Design of Seismic Resistant Steel Frames, Chapmann and Hall, E&FN Spon.

[2] Zandonini R., Bernuzzi C., Bursi O., 1997, "Steel and Steel-Concrete Composite Joints Subjected to Seismic Actions", General report of the STESSA'97 Conference, Kyoto-Japan.

[3] Enghelard M.D., Husain A.S., 1993, "Cyclic-Loading Performance of Welded Flange-Bolted Web Connections", J. of Struct. Eng. ASCE, 119, 12, pp. 3537-3549.

[4] Tsai K.C., Shun W., Popov E., 1995, "Experimental Performance of Seismic Steel Beam-Column Moment Joints", J. of Struct. Eng. ASCE, 121, 6, pp. 925-931.

[5] Plumier A., 1994 "Behaviour of Connections", J. of Constructional Steel Research, vol. 29 pp. 95-119.

[6] Bertero V., Anderson J.C., Krawinkler H, 1997, "Performance of Steel Building Structures during the Northridge Earthquake", EERc, University of California, Berkeley.

[7] Tremblay R., Timler P., Bruneau M., Filiatrault A., 1995, "Performance of Steel Structures during the Northridge Earthquake", Canadian Journal of Civil Engineering, 2,4,Vol.22.

[8] Kuwamura H., Yamamoto K., 1997, "Ductile Crack as Trigger of Brittle Fracture in Steel", J. of Struct. Eng. ASCE, 123, 6, pp. 729-735.

[9] Bernuzzi C., Zandonini R., 1999, "Failure Assessment of Beam-To-Column Steel Joints Via Low-Cycle Fatigue Approaches", The Second International Conference on Advanced in Steel Structures ICASS'99, Volume II, pp.991-998

[10] CEN. Eurocode 3 Part 1-1 "Revised Annex J: joints in building frames. European Commitee for Standardization, 1998.

[11] CEN," Eurocode 8 "Earthquake Resistant Design of Structures", Part 1-1 "General Rules and Rules for Buildings", European Commitee for Standardization, CEN, ENV 1998-2, 1994.

[12] SEAC, "Recommended Lateral Force Requirements and Commentary", Seismology Committee, Structural Engineers Association of California, 1990.

[13] Gruppo Nazionale per la Difesa dai Terremoti (GNDT), "Norme Tecniche per le costruzioni in zone sismiche", Ingegneria Sismica, Addendum, Vol. 2, n. 1, 1985.

[14] Castiglioni C.A., Calado L., 1996, "Comparison of two Cumulative Damage Approaches for the Assessment of Behaviour Factors for Low-rise Steel Buildings", Journal of Constructional Steel Research, Vol. 40, No. 1, pp. 39-61.

[15] Abed A., 2001, "Etude du comportement de structures en profiles mixtes acier-beton partiellement enrobes sommis a l'action sismique", PhD thesis, University of Liege (B), July.

[16] Castiglioni C.A., 1995, "Assessment of Behaviour Factors for Steel Frames based on Linear Elastic Analysis and Cumulative Damage Criteria", 7th Italian Conf. on Seismic Engineering, pp. 589-598

[17] Ballio G., Zandonini R. , 1985, "An experimental equipment to tests steel structural members and subassamblages subjected to cyclic loads", Ingegneria Sismica, Anno III, no. 2.

[18] European Convention for Constructional Steelworks (ECCS), 1986, "Recommended testing procedure for assessing the behaviour of structural elements under cyclic loads", Technical Committee 1, TWG 1.3 - Seismic Design, ECCS Publication No. 45.

[19] Castiglioni C.A., Bernuzzi C. Calado L., Agatino M.R., 1997, "Experimental study on steel beam-to-column joints under cyclic reversal loading", SAC-CUREe, USA, August.

[20] Ballio G., Castiglioni C.A., 1995, "A unified approach for the design of steel structures under low and high cycle fatigue", J. of Constructional Steel Research, vol. 34.

[21] Bernuzzi C., Calado L., Castiglioni C.A., 1997, "Ductility and Load Carrying Capacity Prediction of Steel Beam-to-Column Connections under Cyclic Reversal Loading", J. of Earthquake Engineering, vol. 1, n.2, pp.401-432.

[22] Miner M.A., 1945, "Cumulative Damage in Fatigue", Trans. ASME, J. of Applied Mechanics, Vol. 67, pp.A159-A164.

[23] Castiglioni C.A., 1999, "Failure Criteria and Cumulative Damage Models for steel components under low-cycle fatigue", Proc. XVII C.T.A., Naples, October.

[24] Calado L., Castiglioni C.A., Bernuzzi C., 1997, "Cyclic behaviour of structural steel elements. Method for re-elaboration of test data", Proc. Of the 1st National Colloquium on Steel and composite Construction, Porto, Portugal, Nov., pp. 633-660.